CHARACTERIZING AN ULTRA-HIGH PERFORMANCE MATERIAL FOR BRIDGE APPLICATIONS UNDER EXTREME LOADS

Sri Sritharan, PhD, Iowa State University, Ames, IA
Brant J. Bristow, Iowa State University, Ames, IA
Vic H. Perry, P.Eng., Lafarge North America, Calgary, Canada

ABSTRACT

With an intention of addressing both durability concerns and safety under extreme loads such as earthquakes, research is ongoing at Iowa State University to characterize behavior of a cementituous material composition that can provide the next-generation of structures with ultrahigh performance. The material characterization is performed on a Reactive Powder Concrete (RPC) mix, with the scope of establishing appropriate methods for capturing stress-strain behavior under compression and tension, investigating material behavior under cyclic loading, examining confinement effect on the compression behavior of the material and improving strain capacity of the material. Summarized in this paper are results from the pilot tests, which include the characteristic compression strength, flexural tensile strength, elastic modulus, Poisson's ratio and the effects of cyclic loading.

Keywords: Reactive Powder Concrete, Ductal, Stress-Strain Behavior, Elastic Modulus, Poisson's Ratio, Compressive Strength, Tensile Strength, Cyclic Behavior, Uniaxial Testing

INTRODUCTION

The structural engineering community is currently faced with the challenge of producing long-lasting structures that can perform satisfactorily under service loads in addition to extreme loads such as earthquakes, tornadoes, and blast loads. Clearly, the challenge lies in the ability to address durability issues concurrently with safety and security issues.

All too often, advancements in design result from some sort of catastrophe. Security and structural response to impact loads were issues brought to the forefront in 2001 with the collapse of the World Trade Center towers; significant seismic design advancements occurred after the 1971 San Fernando and 1989 Loma Prieta earthquakes. In-depth research on time-dependent structural behavior became more important after two warehouse roofs at Air Force Bases in Ohio and Georgia cracked and collapsed under combined load, shrinkage, and thermal effects in 1955 and 1956. An issue that may well become a tragic catalyst to structure design advancement is material durability. Many structures, especially bridges, are approaching their useful design life, causing concern for safety even under service loads. Approximately 160,000 substandard large bridges in the United States are crossed an estimated 1 billion times everyday by motorists, according to the Federal Highway Administration (FHWA)[1].

In an attempt to remediate this problem, an underprovided $7 billion is spent annually on upgrading or replacing deteriorated bridges[1,2]. As public demand for mobility without congestion rises, so too does the investment required to address the already deteriorating bridges. Ultrahigh performance materials, including polymer matrix materials (containing glass, carbon, aramid, or thermoplastic fibers), cementitious materials, and high-strength corrosion resistance steel, have been subjects of research over the past decade with the overall objective of improving the condition of civil structures.

Compositions of ultrahigh performance materials have the potential to remediate the durability issues and increase the useful life of structures. However, the solutions based on these materials combined with the conventional design practices will not be compatible with design solutions established for extreme loads, especially earthquakes. The ultrahigh performance materials have high compressive and possibly tensile strengths, but they are very brittle in nature. In contrast, current seismic design practice calls for ductile detailing of critical elements, such as columns in bridges. Regardless of the material strength, these members are required to undergo large inelastic curvature at the section level, which cannot be achieved by incorporating ultrahigh performance materials in conventional design methods.

Ultrahigh performance materials combined with new design techniques can offer future bridges with improved durability without compromising the displacement capacity required by seismic design codes. To support this notion and establish suitable design techniques, an investigation is currently underway at Iowa State University with a focus on material characterization of an ultrahigh performance material. It is envisioned that this study will establish the basic material characteristics necessary for developing new design techniques

that will enable the use of ultrahigh performance materials to address both durability and safety concerns of future structures. This paper presents results of the pilot tests conducted on small scale samples.

MATERIAL AND BENEFITS

A cementitious material known as Reactive Powder Concrete (RPC) has been chosen as the base material for research. Various compositions for RPC have been studied by researchers around the world[3-12]. Typical ranges found for composition of RPC in the literature are given in Table 1 as is the composition chosen for research. Lack of large aggregate, use of silica fume and superplasticizer, and a low water content leads to more uniformly dispersed cement grains and superior overall qualities of RPC over traditional concrete.

Fiber reinforcement content in the range of 1.5 to 2.5% is typically added to RPC to form a fiber-reinforced matrix[4-8]. The steel reinforcing serves to increase the low tensile capacity of RPC, which is characteristic of high strength cementitious materials in general. The study reported in this paper is based on RPC containing 2% (by volume) of short, high strength steel fiber reinforcement.

Table 1: Composition material weights of one cubic foot (meter) of RPC.

Material	Typical Range	Chosen Mix
Water	9 – 12 lb (140 – 195 kg)	8.7 lb (140 kg)
Cement	44 – 61 lb (700 – 980 kg)	44.3 lb (710 kg)
Silica fume	14 – 15 lb (225 – 237 kg)	14.4 lb (230 kg)
Crushed aggregate	13 – 24 lb (210 – 390 kg)	13.1 lb (210 kg)
Fine sand	31 – 66 lb (490 – 1050 kg)	63.7 lb (1020 kg)
Superplasticizer	0.6 – 2.5 lb (10 – 40 kg)	0.8 lb (13 kg)

RPC's qualities include superior strength, self-healing potential due to the significant presence of unreacted cement particles, high-quality surface finish, high penetration resistance, enhanced abrasion resistance, prefabrication capabilities, and superior resistance to de-icing chemicals and the affects of continuous exposure to humid environments. Similar to traditional concrete, RPC can be mixed in a normal, industrial concrete mixer, pumped into forms, placed by buckets, and blended to meet specific structural and/or architectural requirements. Another important feature of RPC is that it can accommodate other advanced materials such as polymers in the design.

Figure 1 compares Scanning Electron Microscope (SEM) images obtained from cured surfaces of regular concrete and RPC matrix containing steel fibers. As seen in Fig. 1b, the particle size in the RPC matrix is kept below 0.025 in. (600 μm), which enables dense

packing of fillers and makes RPC homogeneous and highly impermeable. In comparison to the regular concrete, the number of pores is significantly reduced on the RPC surface. At a magnification of 1000, some pores were found to be interconnected on the regular concrete surface whereas interconnected pores were not found on the RPC surface. The reduced number of and elimination of interconnected pores are primarily responsible for improving durability of the RPC matrix.

The cost of RPC with fiber reinforcement is about ten to twenty times more expensive than traditional concrete. However, prototype projects completed to date suggest that reduced amount of required material due to ultrahigh strengths, reduced labor and maintenance costs resulting from superior qualities, and increased useful life of the structure make the overall project cost comparable to those using traditional concrete.

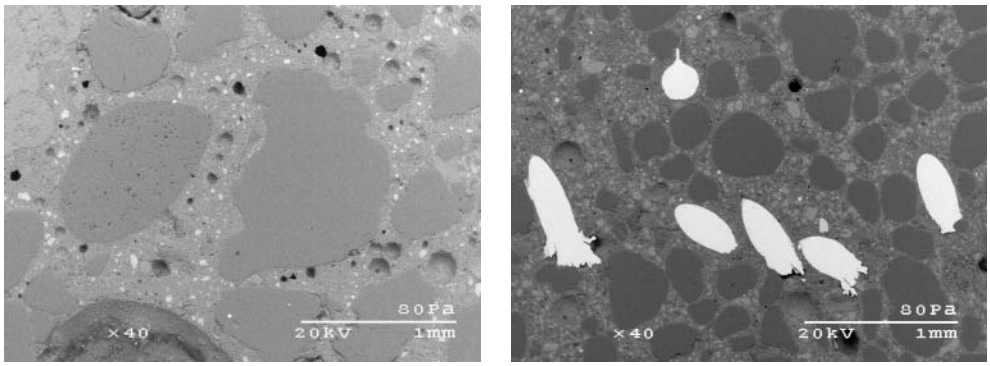

(a) Regular concrete surface (b) RPC surface

Fig. 1: SEM images at 40 times magnification.

SCOPE OF RESEARCH

The scope of the research summarized in this paper is to establish optimal testing procedure and instrumentation setup for uniaxial and cyclic testing of RPC samples under compression and tension loads. In addition to obtaining the loads, strain measurements must be monitored on the samples in the elastic and inelastic ranges. The test procedure should be sufficient to establish engineering properties for design and determine appropriate type and quantity of fibers that can improve strain capacity of RPC, particularly under compression loads.

UNIAXIAL, UNCONFINED COMPRESSION TESTS

MATERIALS AND METHODS

A series of five unconfined compression tests were conducted to develop the optimal testing procedure and instrumentation setup for future compressive testing. These test specimens, and those reported in the subsequent sections, consisted of the RPC mix identified in Table 1

and included 2% of high strength steel fibers (f_y = 360 ksi (2500 MPa), where f_y is the characteristic yield strength). The fibers were 0.008 in. (0.2 mm) in diameter and 0.5 in. (12 mm) long. The samples were prepared by Lafarge North America Inc. and underwent curing and thermal treatment under temperature control, which can be easily performed on large size members at precast plants. The thermal treatment of RPC is known to improve durability properties and time-dependent behavior[4,13]. With the composition of matrix described, the RPC utilized in the tests was identical to a commercially available product known as Ductal®.

The compression test specimens were cylindrical in shape, three in. (75 mm) in diameter and six in. (150 mm) tall. Obtaining accurate measurement of longitudinal strain was one objective of the testing configuration investigated in the pilot study. A simple method of obtaining longitudinal strain is the application of strain gages directly to the test specimen. However, two potential problems may interfere with measurements from strain gages when measuring large strains. In uniaxial compression tests the specimen can potentially bulge or dilate outward (see Fig. 2a, note that the bulging effect has been exaggerated for clarity) due to friction between the ends of test sample and loading plates of the test machine, with the maximum effect occurring toward the mid-height of the specimen. The bulging will result in increased strain gage readings. In compression as well as in other tests, development of localized damage, such as cracking, could also interfere with strain readings or damage the gages. Thus, an alternative means of obtaining longitudinal strain was established to measure average strains over a three-inch (76 mm) length at the mid-height of the sample. In this alternative approach, an aluminum ring attachment consisting of two displacement transducers was used as shown in Figs. 2b and 3a.

The ring attachment consisted of two thin aluminum circular rings spaced along the height of the test specimen. Each ring had three holes, spaced at approximately 120° intervals, so that screws could be used to center the ring on the specimen. The screws were tightened sufficiently against the specimen to prevent slippage. The transducers were positioned on the opposite sides of the specimen and the longitudinal strain was approximated to the average strain obtained from the two transducers.

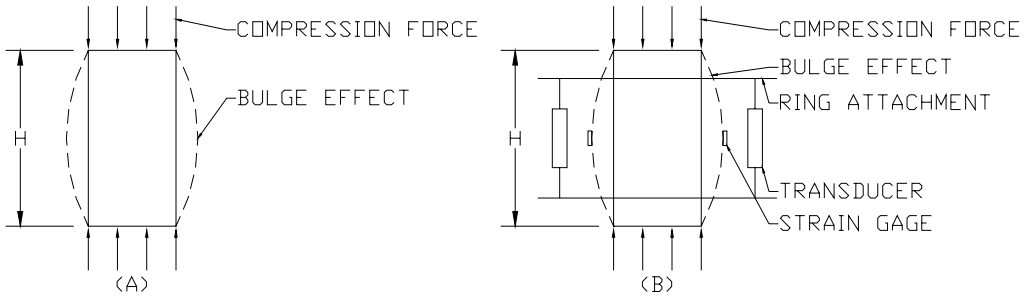

(a) Bulging effect (b) Two methods of instrumentation considered

Fig. 2: Testing under uniaxial compression loads.

Typically, the compression tests were performed with a pair of strain gages and the transducers to measure the longitudinal strain. The hoop strain was monitored in the last three of the five tests using two strain gages mounted at the mid-height, on opposing sides of the specimen. Figure 3b shows two samples after failure in uniaxial compression.

(a) Test setup

(b) Samples after failure

Fig. 3: Compression test of RPC sample, including ring attachment.

RESULTS AND DISCUSSION

Stress versus strain plots were made for each test, comparing the average longitudinal strain data from transducers and strain gages as a function of compressive stress. Figure 4 shows an example using data obtained in Test 5. The plots in this and other similar figures are typically limited to the undisturbed portions, which do not include the maximum stress recorded during the test. At the maximum strength, sporadic disturbance to the instrumentation data were obvious as test samples began to fail, which is seen for data obtained from strain gages in Fig. 4. As can be seen in this figure, both devices gave similar values up to a strain of 0.0015, but strain gage data deviated from a linear trend at strains greater than 0.0015.

Figure 5 displays the stress-strain curves obtained from several unconfined compression tests, in which the strains were based on the transducer data. Satisfactory attachment of the rings to the specimens was also investigated in this series of tests. As can been seen, the procedure adopted for the first two tests was unsatisfactory, resulting in deviation from a linear trend at large strains. Tests 3 – 5 results compare with each other satisfactorily and show linear response until close to failure. From the strain measured at 45% of the compressive strength and by fitting a straight line through data points, an elastic modulus, E_{RPC}, for the RPC matrix was determined to be 8000 ksi. This information and other material properties established from these tests are reported in Table 2. Though preliminary, the data indicated that E_{RPC} may be satisfactorily approximated as:

$$E_{RPC} = 50{,}000\sqrt{f'_c(\text{psi})} = 4200\sqrt{f'_c(\text{MPa})} \quad (1)$$

where f'_c is the unconfined compressive strength of the RPC matrix.

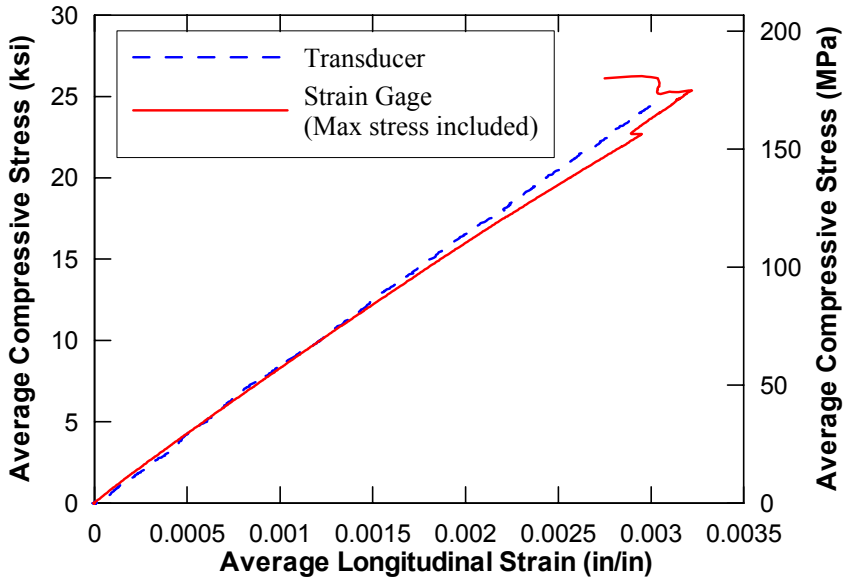

Fig. 4: Compressive stress-strain plots obtained from Test 5.

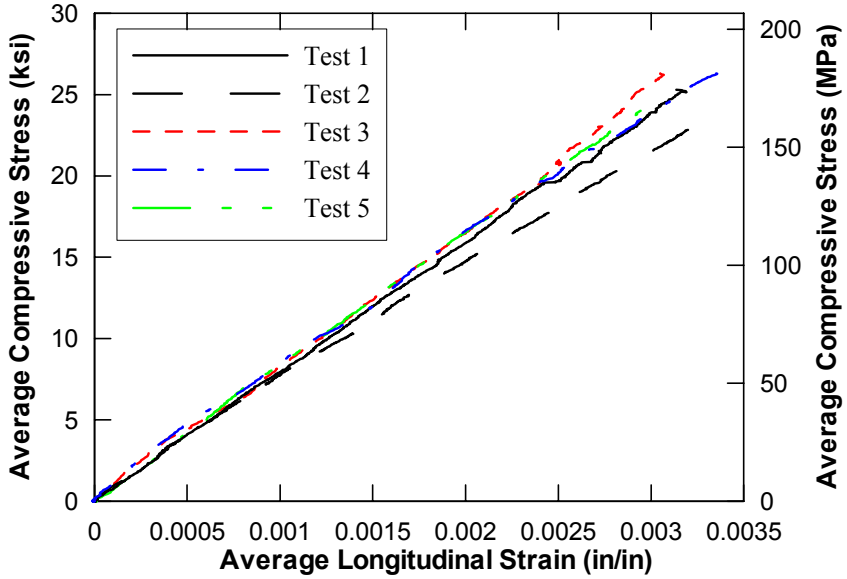

Fig. 5: Compressive stress-strain plots established from transducer data.

As previously noted, hoop strain resulting from dilatation in the transverse direction was measured at mid-height of the samples in Tests 3 – 5. Average hoop strains measured in

these tests are shown as a function of longitudinal strains in Fig. 6. These data resulted in Poisson's ratios in the range of 0.17 – 0.2, with an average value of 0.18. This is comparable to the average range of 0.15 – 0.2 found for traditional concrete[14].

Table 2: Engineering properties of RPC including 2% steel fibers.

Parameter	Average Value
Linear elastic limit of longitudinal strain, ε_c	0.0032 in/in
Compressive strength, f'_c	25.6 ksi (177 MPa)
Elastic modulus, E_{RPC}	8000 ksi (55 GPa)
Poisson's ratio, ν	0.18

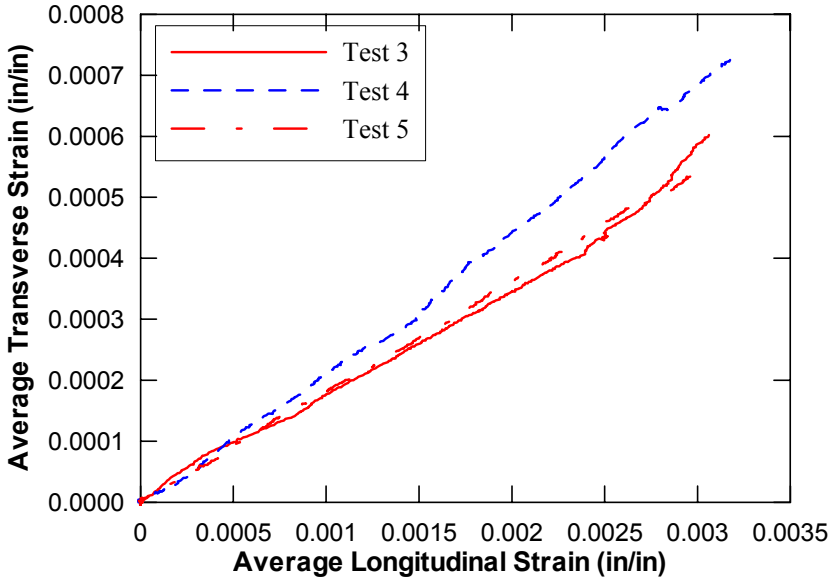

Fig. 6: Transverse strain versus longitudinal strain from transducer data.

UNIAXIAL, CONFINED COMPRESSION TEST

MATERIALS AND METHODS

An attempt was made to perform a compression test with high confinement. For a test cylinder, similar in material composition and size to those used in unconfined compression tests, confinement was added externally using a 1/8 in. (3.2 mm) thick circular steel tube. Accounting for a gap of 5/8 in. (16 mm) between the tube and ends of the test cylinder in the vertical direction, the test cylinder was subjected to an average confining pressure of about 2 ksi (13.8 MPa). In the radial direction, a 3/16 in. (4.8 mm) gap was purposely left between the steel tube and the test cylinder, which was filled using a high strength plaster material (f'_c

= 18 ksi (124 MPa)). Longitudinal strain was measured by connecting the ring attachment directly to the RPC cylinder while the hoop strain was monitored at mid-height using strain gages placed on the tube.

RESULTS AND DISCUSSION

Figure 7 shows the average longitudinal strain as a function of compressive stress obtained from the confined compression test, referred to as Test 6. The measured ultimate strength of confined sample was 35.8 ksi (247 MPa). A linear stress-strain curve is apparent with approximately the same linearity as that established for unconfined compression tests. The maximum longitudinal strain measured at the end of the most linear portion of the confined concrete stress versus strain plot was 0.0039, which was about 125% higher than the average value measured in the unconfined tests. This increase in strain capacity was relatively small given the average confining pressure.

Although the values were relatively small in comparison to the unconfined tests, the hoop strain was found to be significant and resulted in a Poisson's ratio of 0.15. This indicated that the method employed for confining the sample was not fully effective, presumably due to the deformation of the high-strength plaster used to fill the gap between confining steel tube and the test cylinder. Furthermore, an analysis of the failure surface of unconfined samples under SEM revealed that the steel fibers oriented in the radial direction experienced fracture and that the confined behavior of the RPC matrix could be improved. Therefore, it was concluded that a series of confinement tests with and without external confinement would be valuable. In these tests, the type and quantity of fibers and the amount of external confinement will be the main variables. To improve effectiveness of external confinement, the RPC will be cast inside steel tubes.

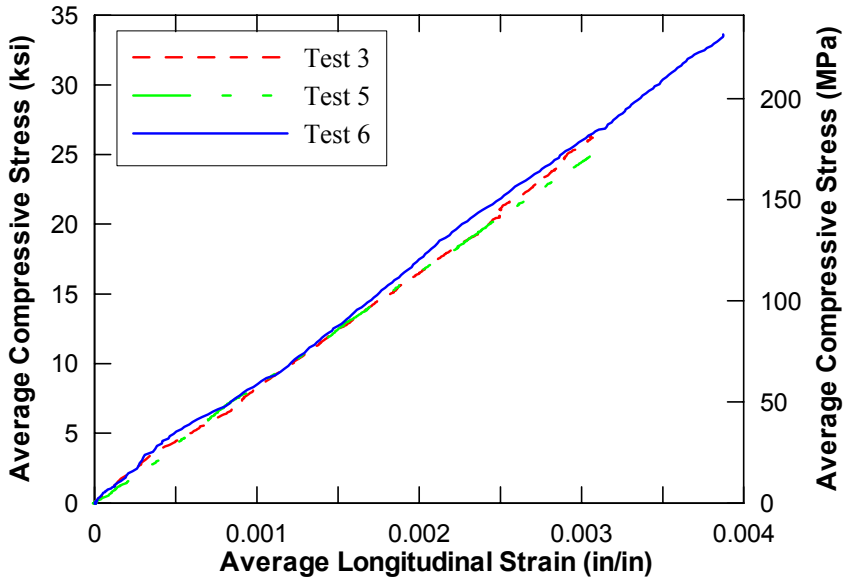

Fig. 7: Compressive stress-strain plot for confined and unconfined test data.

CYCLIC COMPRESSION TESTS

MATERIALS AND METHODS

Due to the possibility of developing micro-cracks, there is potential for strength degradation of RPC samples in the elastic range. To investigate this concern, a series of large-amplitude low-cycle fatigue compressive tests were performed within an elastic strain limit of ε_c. Three-inch (75 mm) diameter, six-inch (150 mm) tall cylindrical specimens without confinement were used in these tests. The material composition of RPC was as previously described but from a different batch.

Four tests have been completed as part of an ongoing investigation. The first test (CC1) was a standard, monotonic compression test to establish the maximum compressive stress (f'_c) and the linear elastic strain limit (ε_c) for the samples. The three cyclic compression tests (CC2, CC3, and CC4) are graphically represented in Fig. 8. Loading on CC2 consisted of eleven loading steps, from 0.1 ε_c to 1.0 ε_c (as seen in Fig. 8), with a final step loading the specimen until failure. Loading for CC3 was the same as that for CC2, but three cycles were imposed at each loading step (Fig. 8a). CC4 was loaded the same as CC2, but had an initial loading step of 0.7ε_c and then proceeded from 0.1 ε_c to 1.0 ε_c to failure (Fig. 8b).

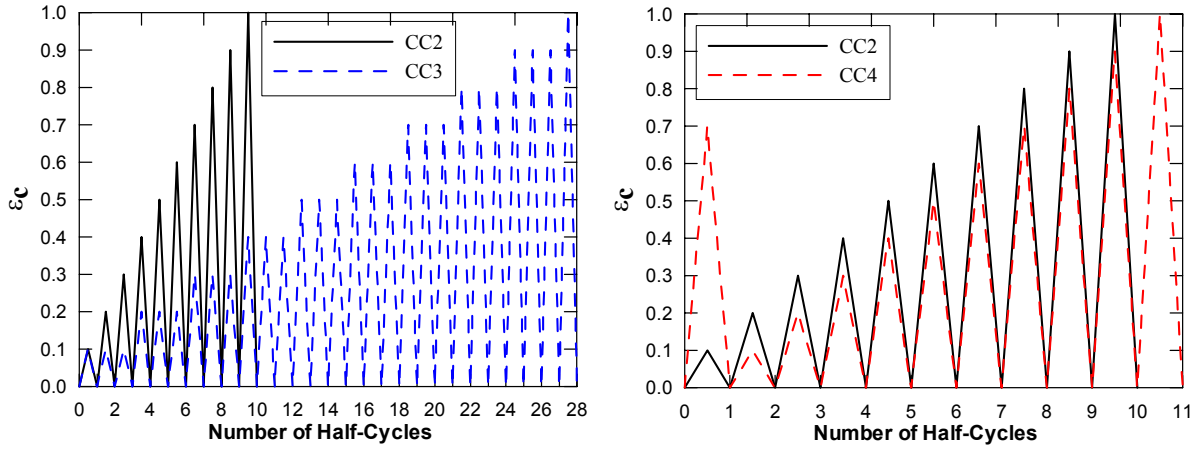

(a) Comparison of CC2 and CC3 (b) Comparison of CC2 and CC4

Fig. 8: Loading patterns chosen for cyclic compression tests.

RESULTS AND DISCUSSION

The f'_c and ε_c values determined from CC1 as the basis for the cyclic tests were 23 ksi (159 MPa) and 0.0034, respectively. Stress-strain plots for the cyclic tests did not show any significant degradation due to large-amplitude elastic strain cycles. To illustrate this observation, the stress-strain plots obtained from an unconfined compression test from the previous batch (Test 5), the monotonic compression test (CC1), and individual peaks obtained at the different strain levels in the first load cycle for CC3 are shown in Fig. 9. The

linear trend exhibited by the material under monotonic load is also visible for the cyclic load data until large strains are reached. An insignificant amount of deviation from the linear trend is visible at strains above 0.002. In addition to confirming the material behavior, Fig. 9 verifies satisfactory performance of the ring attachment under cyclic compression loads. From the monotonic loading of CC2, CC3, and CC4 performed at the conclusion of the cyclic loads, an average compressive strength of 26 ksi (180 MPa) was obtained, indicating no effects of the cyclic loading on the ultimate strength of the cylinders.

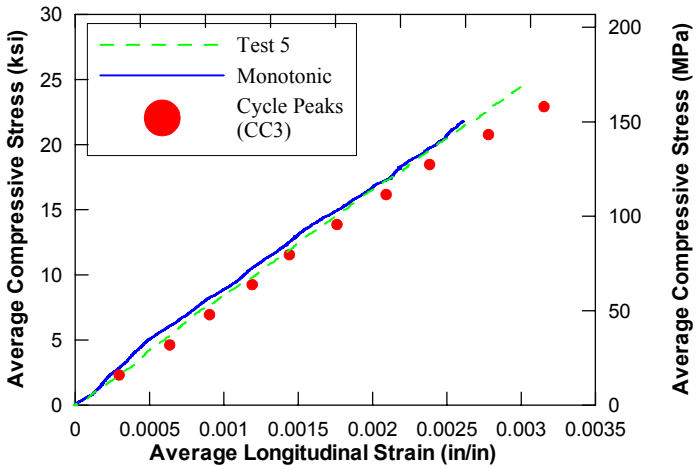

Fig. 9: Stress-strain plot showing unconfined (Test 5) and monotonic (CC1) test results with first load cycle peaks for CC3.

FLEXURAL TENSION TESTS

MATERIALS AND METHODS

Four flexural tests (BM1 – BM4) were conducted on small-size samples to examine toughness (ductility) of the material and verify the flexural tension capacity. The 6.3 in. (160 mm) long test specimens had a 1.6 in. x 1.6 in. (40 mm x 40 mm) square cross-section. They were simply supported approximately at 0.5 in. (12.7 mm) from the ends and were subjected to two-point loading over an average distance of 2 in. (51 mm) across the mid span (see Fig. 10a). Flexural compressive and tensile strains were measured in the constant bending region by affixing two strain gages to the top and bottom surfaces of the specimens. All specimens were subjected to monotonic loading, except BM4 in which loads were almost completely removed and reloaded at specified strain levels.

RESULTS AND DISCUSSION

The test units exhibited linear behavior until developing a tensile stress of about 3 ksi (21 MPa), beyond which inelastic responses were observed. At this limit of linear behavior, strains at the extreme tension and compression fiber were 0.000321 and 0.000282, respectively. This indicated that the effective moment of inertia (I_e) of the beam in the linear

elastic region was 0.85 I_g, where I_g is the gross moment of inertia; the location of the neutral axis was also noted to have moved from the mid-depth up to 38% of the beam depth. Although no flexural cracks were observed, the reduction in the moment of inertia in the linear elastic range is believed to be due to microcracking. Traditional reinforced concrete beams exhibit $I_e = 0.4\ I_g$ prior to yielding of the longitudinal reinforcement, which is due to the formation of flexural cracking[14].

Figure 10b shows two test beams after failure, which was initiated by the formation of a localized single crack. The failure load of the beams indicated an average flexural tensile strength of 4.9 ksi (34 MPa). The maximum recorded compressive strain at the ultimate strength was in the range of 0.0015 to 0.0024. Since these strains are about 48 – 75% of the linear elastic strain limit established from the uniaxial, unconfined compression tests, it was concluded that by incorporating supplemental tension reinforcement in the critical regions, the flexural ductility capacity of the RPC members could be improved. Figure 11 shows the bending stress versus compressive strain plots obtained for BM3 and BM4, and demonstrates the range of maximum strains exhibited by the beam samples. The unloading cycles imposed on BM4 show the potential for hysteresis action of RPC members in the inelastic region. With added reinforcement, the energy dissipating ability of the RPC members could also be improved.

(a) Test setup (b) Samples after failure

Fig. 10: Flexural testing of small beams.

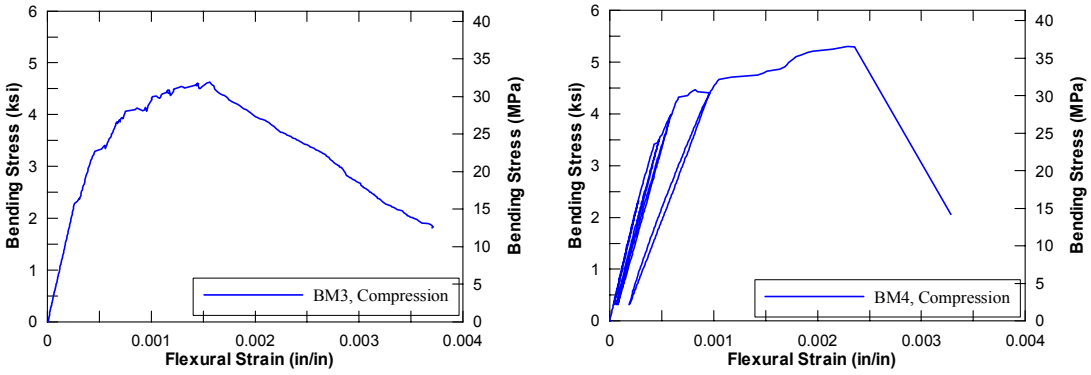

(a) Compression results of BM3 (b) Compression results of BM4

Fig. 11: Stress-strain plots obtained from flexural beam tests.

CONCLUSIONS

Results obtained from a series of pilot tests conducted on small-size test specimens made from a Reactive Powder Concrete (RPC) matrix consisting of 2% high strength steel fibers is summarized in this paper. The unconfined, uniaxial tests indicated an ultimate compressive strength of 25.6 ksi (177 MPa) for the RPC mix. The relationship between elastic modulus and unconfined compressive strength was found to be fairly comparable to that established for traditional concrete. As a result, the elastic modulus of RPC with a compressive strength of 25.6 ksi (176 MPa) is about twice that of regular concrete with 5 ksi (34.5 MPa) compressive strength. Poisson's ratio of the RPC matrix was comparable to the average range reported for regular concrete. The material behavior under uniaxial compression was linear up to a compression strain of 0.0032. A compression test was performed with a high amount of external confinement. Though increases in the ultimate strength and strain limit were observed, it was concluded the test was not fully effective due to the deformation that occurred to the high-strength plaster used to fill the gap between the confining steel tube and test cylinder. A series of confinement tests will be conducted in the near future, in which the plaster will be eliminated by casting samples inside steel tubes.

The influence that micro-cracks may have on cyclic response was investigated within the elastic range by subjecting three cylinders to cyclic compression loads. The responses were repeatable at the peak strains, concluding that strength degradation should not occur due to large amplitude elastic strain cycles.

The flexural behavior of RPC was investigated through testing of small-size beams, which showed an effective moment of inertia equal to 85% of the gross moment of inertia, movement of the neutral axis depth up from the midheight of the beam to 38% of the beam depth, and an average flexural tensile strength of 4.9 ksi (34 MPa). Furthermore, through limited cycling of the load on one specimen, the energy dissipation potential was examined. For application of RPC in members that may be subjected to large curvature at the section level due to extreme loads, consideration of supplemental reinforcement in the critical regions seems appropriate. The supplemental reinforcement will increase the curvature capacity of the section while delaying the formation of large localized cracks and providing additional hysteretic damping.

ACKNOWLEDGEMENTS

The results summarized in this paper are from a preliminary investigation conducted on an ultrahigh performance material at Iowa State University (ISU) in collaboration with Lafarge North America, Inc. The authors thank Terry Chow and Gavin Geist of Lafarge North America for coordination and preparation of the test samples and Mr. Douglas Wood of ISU for his assistance with testing of the samples.

REFERENCES

1. Chase, S. B., "FHWA's Research and Technology Vision for the Future," *Proceedings of the 18th US-Japan Bridge Engineering Workshop*, (St. Louis, Missouri), Oct. 2002, pp. 26-33.
2. Office of Infrastructure, "Delivering Infrastructure for America's Future," Technical Brochure, Publication No. FHWA-RD-02-091, Federal Highway Administration, U.S. Department of Transportation.
3. Yang, Y., "Manufacturing Reactive Powder Concrete Using Common New Zealand Materials," Dept. of Civil and Resource Engineering, University of Auckland, New Zealand, Report No. 598, July 2000.
4. Bonneau, O., Lachemi, M., Dallaire, E., Dugat, J., Aitcin, P. C., "Mechanical Properties and Durability of Two Industrial Reactive Powder Concrete," *ACI Materials Journal*, V. 94, No. 4, July-Aug. 1997, pp. 286-290.
5. Richard, P., Cheyrezy, M. H., "Reactive Powder Concretes with High Ductility and 200-800 MPa Compressive Strength," *Concrete Technology: Past, Present, and Future, Preceedings of V. Mohan Malhotra Symposium,* ed. Wieczorek, V. (Detroit, Michigan), ACI SP-144, March 1994, pp. 507-518.
6. Dugat, J., Roux, N., Bernier, G., "Mechanical Properties of Reactive Powder Concretes," *Materials and Structures/Materiaux et Constructions*, V. 29, No. 188, May 1996, pp. 233-240.
7. Collepardi, S., Coppola, L., Troli, R., Collepardi, M., "Mechanical Properties of Modified Reactive Powder Concrete," *Superplasticizers and Other Chemical Admixtures in Concrete. Proceedings Fifth CANMENT/ACI International Conference*, ed. Malhotra, V. M. (Rome, Italy), ACI SP-173, 1997, pp. 1-21.
8. Campbell, R. L., Sr., Edward F. O'Neil, Dowd, W. M., Dauriac, C. E., "Reactive Powder Concrete for Producing Sewer, Culvert, and Pressure Pipes," *US Army Engineer Waterways Experiment Station*, Technical Report, CPAR-SL-98-3, Aug. 1998.
9. Roux, N., Andrade, C., Sanjuan, M. A., "Experimental Study of Durability of Reactive Powder Concretes," *Journal of Materials in Civil Engineering*, V. 8, No. 1, Feb. 1996, pp. 1-6.
10. Matte, V., Moranville, M., "Durability of Reactive Powder Composites: Influence of Silica Fume on the Leaching Properties of Very Low Water/binder Pastes," *Cement and Concrete Composites*, V. 21, No. 1, Feb. 1999, pp. 1-9.
11. Feylessoufi, A., Villieras, F., Michot, L. J., DeDonato, P., Cases, J. M., Richard, P., "Water Environment and Nanostructural Network in a Reactive Powder Concrete," *Cement and Concrete Composites*, V. 18, No. 1, Jan. 1996, pp. 23-29.
12. Bonneau, O., Poulin, C., Dugat, J., Richard, P., Aitcin, P. C., "Reactive Powder Concretes: from Theory to Practice," *Concrete International*, V. 18, No. 4, April 1996, pp. 47-49.
13. Hartman, J. and Graybeal, B., "Testing of Ultra-high Performance Concrete Girders," *PCI Journal*, V. 47, No. 1, 2002, pp. 148-149.
14. Park, R. and Paulay, T. Reinforced Concrete Structures. New York: Wiley-Interscience, 1975.